Synthesis, Characterization, and Photochemical Properties of Azobenzene-Conjugated Ru(II) and Rh(III) Bis(Terpyridine) Complexes

Tomona Yutaka,[†] Ichiro Mori,[†] Masato Kurihara,[†] Jun Mizutani,[†] Kenya Kubo,[†] Sanae Furusho,[‡] Kazuo Matsumura,[§] Naoto Tamai,[§] and Hiroshi Nishihara*[,†]

Department of Chemistry, School of Science, The University of Tokyo, 7-3-1 Hongo, Bunkyo-ku, Tokyo 113-0033, Japan, Jasco International, Co., Ltd., 1-11-10 Myojin-cho, Hachioji, Tokyo 192-0046, Japan, and Department of Chemistry, Faculty of Science, Kwansei Gakuin University, 1-1-155 Uegahara, Nishinomiya, Hyogo 662-8501, Japan

Received March 29, 2001

We synthesized azobenzene-conjugated bis(terpyridine) Ru(II) and Rh(III) mononuclear and dinuclear complexes and investigated their photochemical properties on excitation of the azo $\pi-\pi^*$ band upon 366 nm light irradiation. The Ru mononuclear complex underwent trans-to-cis photoisomerization to reach the photostationary state with only 20% of the cis form, while the Ru dinuclear complex did not isomerize at all photochemically. On the other hand, the mononuclear and dinuclear Rh complexes showed almost complete trans-to-cis photoisomerization behavior. Cis forms of the Rh complexes thermally returned to the trans form at a much slower rate than those of organic azobenzenes, but they did not isomerize photochemically. The reduction potential of the cis forms was 80 mV more negative than that of the trans forms. The photoisomerization quantum yields of the Rh complexes were strongly dependent on the polarity, viscosity, and donor site of the solvents as well as the size of the counterions. We investigated the photoisomerization process of these complexes using femtosecond absorption spectroscopy. For the Rh complexes, we observed $S_n \leftarrow S_2$ and $S_n \leftarrow S_1$ absorption bands similar to those of organic azobenzenes. For the Ru complexes, we observed very fast bleaching of the MLCT band of the Ru complex, which indicated that the energy transfer pathway to the MLCT was the primary cause of the depressed photoisomerization. The electronic structures, which were estimated from ZINDO molecular orbital calculation, supported the different photochemical reaction behavior between the Ru and Rh complexes.

Introduction

Transition-metal polypyridine complexes have recently attracted much attention because of their unique photochemical and electrochemical properties depending on the metal.[1] In contrast to tris(bipyridine) complexes, bis(terpyridine) complexes have the advantage of the possibility of constructing single-component octahedral complex oligomers because they have no geometric isomers. Connecting the two terpyridine moieties with a π-conjugated spacer at their 4′ positions affords linear π-conjugated multinuclear complexes. There have been many reports on the assemblies of bis(terpyridine) complexes, in most cases examining photoinduced electron- or energy-transfer reactions.[2]

The azo group is known to undergo reversible trans−cis transformation, especially in azobenzene and its derivatives,[3−5] and it also acts as a π-conjugated spacer when it is inserted between two complex units. If bis(terpyridine) complex units are connected with an azobenzene as the spacer group, the products are expected to have photochemically changeable structure and properties. Only a few reports are available on azo-bridged metal complexes,[6,7] while numerous publications have appeared regarding the isomerization of organic azoben-

* To whom correspondence should be sent.
[†] The University of Tokyo.
[‡] Jasco International, Co., Ltd.
[§] Kwansei Gakuin University.

(1) (a) Constable, E. C.; Thompson, A. M. W. C.; Tochter, D. A.; Daniels, M. A. M. *New J. Chem.* **1992**, *16*, 855. (b) Constable, E. C.; Thompson, A. M. W. C. *J. Chem. Soc., Dalton Trans.* **1992**, 2947. (c) Hadda, T. B.; Bozec, H. L. *Inorg. Chim. Acta* **1993**, *204*, 103. (d) Binstead, R. A.; Stulta, L. K.; Meyer, T. J. *Inorg. Chem.* **1995**, *34*, 546. (e) Maestri, M.; Armaroli, N.; Balzani, V.; Constable, E. C.; Thompson, A. M. W. C. *Inorg. Chem.* **1995**, *34*, 2759. (f) Fagalde, F.; Katz, N. D. L.; Katz, N. E. *Polyhedron* **1997**, *16*, 1921. (g) Storrier, G. D.; Colbran, S. B.; Craig, D. C. *J. Chem. Soc., Dalton Trans.* **1998**, 1351. (h) Pramanik, N. C.; Pramanik, K.; Ghosh, P.; Bhattacharya, S. *Polyhedron* **1998**, *17*, 1525.

(2) (a) Constable, E. C.; Thompson, A. M. W. C. *J. Chem. Soc., Dalton Trans.* **1992**, 3467. (b) Whittle, B.; Everest, N. S.; Howard, C.; Ward, M. D. *Inorg. Chem.* **1995**, *34*, 2025. (c) Sauvage, J. −P.; Collin, J. −P.; Chambron, J. −C.; Guillerez. S.; Coudret, C. *Chem. Rev.* **1994**, *94*, 993. (d) Constable, E. C.; Thompson, A. M. W. C. *New J. Chem.* **1996**, *20*, 65. (e) Indelli, M. T.; Scandola, F.; Flamigni, L.; Collin, J.-P.; Sauvage, J.-P.; Sour, A. *Inorg. Chem.* **1997**, *36*, 4247. (f) Storrier, G. D.; Colbran, S. B.; Craig, D. C. *J. Chem. Soc., Dalton Trans.* **1997**, 3011. (g) Collin, J. −P.; Gavina, P.; Heitz, V.; Sauvage, J. -P. *Eur. J. Inorg. Chem.* **1998**, 1. (h) Lee, J.-D.; Vrana, L. M.; Bullock, E. R.; Brewer, K. J. *Inorg. Chem.* **1998**, *37*, 3575. (i) Janini, T. E.; Fattore, J. L.; Mohler, D. L. *J. Organomet. Chem.* **1999**, *578*, 260. (j) Kelch, S.; Rehahn, M. *Macromolecules* **1999**, *32*, 5818.

(3) (a) Rau, H.; In *Photochromism. Molecules and Systems*; Dürr, H. B., -Laurent, H., Eds.; Elsevier: Amsterdam, 1990; p. 165. (b) Junge, D. M.; McGrath, D. V. *J. Chem. Soc., Chem. Commun.* **1997**, 857. (c) Röttger, D.; Rau, H. *J. Photochem. Photobiol. A* **1999**, *101*, 205. (d) Yamaguchi, T.; Nakazumi, H.; Irie, M. *Bull. Chem. Soc. Jpn.* **1999**, *72*, 1623. (e) Feringa, B. L.; Delden, R. A. von.; Koumura, N.; Geertsema, E. M. *Chem. Rev.* **2000**, *100*, 1789.

(4) (a) Sekkat. Z.; Wood, J.; Knoll, W. *J. Phys. Chem.* **1995**, *99*, 17226. (b) Cimiraglia, R.; Asano, T.; Hofmann, H.-J. *Gazz. Chim. Ital.* **1996**, *126*, 679. (c) Sanchez. A. M.; de Rossi, R. H. *J. Org. Chem.* **1996**, *61*, 3446. (d) Lednev, I. K.; Ye, T. -Q.; Hester, R. E.; Moore, J. N. *J. Phys. Chem.* **1996**, *100*, 13338. (e) Cattaneo, P.; Persico, M. *Phys. Chem. Chem. Phys.* **1999**, *1*, 4739. (f) Sanchez, A. M.; Barra, M.; de Rossi, R. H. *J. Org. Chem.* **1999**, *64*, 1604. (g) Tamai, N.; Miyasaka, H. *Chem. Rev.* **2000**, *100*, 1875.

10.1021/ic010351u CCC: $20.00
Published on Web 08/15/2001

zenes[3] as well as their mechanism[4] and application.[5] Furthermore, the photoisomerization behavior of the metal complexes has been discussed in limited studies[6] and, in others, the azo group has been utilized only as a π-conjugated spacer.[7] This is probably because the conditions of photoisomerization are more restricted for the complexes with more intricate energy levels than for simple organic azobenzenes and/or because photoisomerization is suppressed by the energy transfer from the azo chromophore to the metal centers.[8]

We have synthesized an azobenzene-bridged bis(terpyridine) ligand (tpy-AB-tpy) and its Ru(II) and Rh(III) dinuclear complexes and investigated their photochemical properties.[8] The aim of our study is to clarify the factors regulating the isomerization of the azo-bridged metal complexes and to control the electronic interaction between the metal centers affecting internuclear energy transfer or electron transfer in response to the isomerization. With regard to organic azobenzenes, it has been reported that the quantum yield of trans-to-cis photoisomerization increases, and that of cis-to-trans photoisomerization decreases in more polar solvent.[9a] The cis-to-trans thermal isomerization rate also depends on the solvent and functional groups attached to the azobenzene molecules, especially for push−pull substituted asymmetric azobenzenes.[9b−g] The preliminary results of our studies have shown that the photoisomerization of the Ru(II) complex is depressed by energy transfer,[8a] whereas the trans-to-cis photoisomerization of the Rh(III) complexes proceeds and their photoisomerization rate is dependent on the nature of the solvent and the counterions.[8b] Here, we present the physical properties of various Ru(II) and Rh(III) complexes and additional photoisomerization behavior dependent on the metal center, solvents, and counterions. We have also synthesized mononuclear complexes containing an azobenzene-attached terpyridine ligand (tpy-AB) and compared their properties with those of dinuclear complexes. Differences in the femtosecond transient spectroscopy and molecular orbital diagrams between the Ru(II) and Rh(III) complexes are also described in this paper.

Chart 1

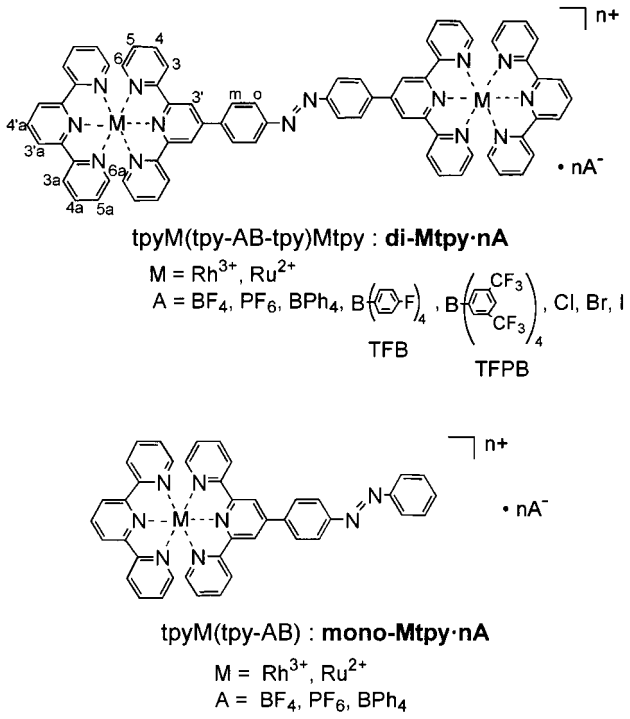

Experimental Section

Materials. 4′-(4-Anilino)-2,2′:6′,2″-terpyridine,[2f,8a] nitrosobenzene,[10] tpy-AB-tpy,[8a] and $RhCl_3tpy$[11] were prepared according to the literature. Rhodium trichloride (Furuya Metals), sodium tetrakis(4-fluorophenyl)-borate (Na^+TFB^-, Tokyo Kasei), sodium tetrakis{3,5-bis(trifluoromethyl)-phenyl}borate dihydrate (Na^+TFPB^-, Dojin), tetrabutylammonium chloride (Acros Organics), and other reagents and solvents purchased from Kanto Chemicals were used as received. Guaranteed-grade solvents (Kanto Chemicals) and spectroscopic-grade acetonitrile (Kanto Chemicals) were used for UV−vis absorption spectroscopy. Acetonitrile used for the electrochemical measurements was of HPLC grade (Kanto Chemicals). Tetrabutylammonium tetrafluoroborate (lithium-battery grade) for the electrochemical measurements was obtained from Tomiyama Chemicals.

Caution: Nitrosobenzene is harmful and must be stored in a refrigerator because it has a very high vapor pressure at room temperature.

Apparatus. UV−vis, IR, ^{1}H NMR, and FAB mass spectra were recorded with Jasco V-570 and Hewlett-Packard 8453 UV−vis spectrometers, a Jasco FT/IR-620v spectrometer, JEOL EX270 and Brucker AM 500 spectrometers, and a JEOL JMS−SX102 spectrometer, respectively. Photoisomerization measurements were carried out under a nitrogen atmosphere using a USHIO 500W super high-pressure mercury lamp USH-500D as an irradiation source. The 366-nm light was isolated with a UV-D35 Toshiba band-pass filter. The 430-, 440-, and 450-nm lights were isolated with KL-43, KL-44, and KL-45 Toshiba interference filters, respectively.

Electron Spray Ionization (ESI) Mass Spectrometry Measurements. ESI mass spectra (ESI MS) were obtained with a Micromass LCT (time-of-flight mass spectrometer). Each sample was infused as an acetonitrile−H_2O solution (8:2 v/v), except for an acetonitrile−H_2O solution (5:5 v/v) for the halide salts of the Rh complexes, because of the low solubility of halide salts in acetonitrile. Cone voltage was varied

(5) (a) Kumar, G.; Necker, D. C. *Chem. Rev.* **1989**, *89*, 1915. (b) Ikeda, T.; Sasaki, T.; Ichimura, K. *Nature* **1993**, *361*, 428. (c) Anzai, J.; Osa. T. *Tetrahedron* **1994**, *42*, 67. (d) Ikeda, T.; Tsutsumi, O. *Science* **1995**, *268*, 1873. (e) Osman, P.; Martin, S.; Milojevtic, D.; Tansey C. *Langmuir* **1998**, *14*, 4238. (f) Archit, A.; Vögtle, F.; De Cola, L.; Azzellini, G. C.; Balzani, V.; Ramanujam, P. S.; Berg, R. H. *Chem. Eur. J.* **1998**, *4*, 699. (g) Delaire, J. A.; Nakatani K. *Chem. Rev.* **2000** *100*, 1817. (h) Ichimura, K. *Chem. Rev.* **2000**, *100*, 1847.

(6) (a) Hayami, S.; Inoue, K.; Osaki, S.; Maeda, Y. *Chem. Lett.* **1998**, 987. (b) Yam, V. W. -W. Y.; Lau, V. C. -Y.; Wu, L. -X. *J. Chem. Soc., Dalton. Trans.* **1998**, 1461. (c) Tsuchiya, S. *J. Am. Chem. Soc.* **1999**, *121*, 48. (d) Aiello, I.; Ghedini, M.; La Deda, M.; Pucci, D.; Francescangeli, O. *Eur. J. Inorg. Chem.* **1999**, 1367.

(7) (a) Das, A.; Maher, J. P.; McCleverty, J. A.; Badiola, J. A. N.; Ward, M. D. *J. Chem. Soc., Dalton. Trans.* **1993**, 681. (b) Otsuki, J.; Sato, K.; Tsujino, M.; Okuda, N.; Araki, K.; Seno, M. *Chem. Lett.* **1996**, 847. (c) Otsuki, J.; Tsujino, M.; Iizaki, T.; Araki, K.; Seno, M.; Takatera, K.; Watanabe, T. *J. Am. Chem. Soc.* **1997**, *119*, 7895. (d) Kurihara, M.; Kurosawa, M.; Matsuda. T.; Nishihara, H. *Synth. Metals* **1999**, *102*, 1517. (e) Kurosawa, M.; Nankawa, T.; Matsuda. T.; Kubo, K.; Kurihara, M.; Nishihara, H. *Inorg. Chem.* **1999**, *38*, 5113. (f) Noro, S.; Kondo, M.; Ishii, T.; Kitagawa, S.; Matsuzaka, H. *J. Chem. Soc., Dalton Trans.* **1999**, 1569. (g) Sun, S. −S.; Lees, A. J. *J. Am. Chem. Soc.* **2000**, *122*, 8956. (h) Mosher, P. J.; Yap, G. P. A.; Crutchley, R. J. *Inorg. Chem.* **2001**, *40*, 1189.

(8) (a) Yutaka, T.; Kurihara, M.; Nishihara, H. *Mol. Cryst. Liq. Cryst.* **2000**, *343*, 193. (b) Yutaka, T.; Kurihara, M.; Kubo, K.; Nishihara, H. *Inorg. Chem.* **2000**, *39*, 3438.

(9) (a) Bortolus, P.; Monti, S. *J. Phys. Chem.* **1979**, *83*, 648. (b) Halpern, J.; Brady, G. W.; Winkler, C. A. *Can. J. Res. Sec. B* **1950**, *28*, 140. (c) Le Fèvre, J. W.; Northcott, J. *J. Chem. Soc.* **1953**, 867. (d) Wildes, P. D.; Pacifici, J. G.; Irick, G., Jr.; Whitten, D. G. *J. Am. Chem. Soc.* **1970**, *93*, 2004. (e) Asano, T.; Okada, T. *J. Org. Chem.* **1984**, *49*, 4387. (f) Nishimura, N.; Kosako, S.; Sueishi, Y. *Bull. Chem. Soc. Jpn.* **1984**, *57*, 1617. (g) Asano, T.; Okada, T. *J. Org. Chem.* **1986**, *51*, 4454.

(10) Coleman, G. H.; McCloskey, C. M.; Stuart, F. A. *Org. Synth.* Coll. Vol. *3*, 688.

(11) Odobel, F.; Sauvage, J. -P.; Harriman, A. *Tetrahedron Lett.* **1993**, *34*, 8113.

in the range of 30 to 60 V to obtain clear peaks, but the intensities and patterns in the spectra were not essentially changed within this range.

Electrochemical Measurements. A glassy carbon rod (diameter 5 mm; Tokai Carbon GC-20) was embedded in Pyrex glass, and the cross-section was used as a working electrode. Cyclic voltammetry measurements were carried out in a standard one-compartment cell under Ar equipped with a platinum-wire counter electrode and an Ag/Ag^+ reference electrode with a BAS CV-50W voltammetric analyzer.

Determination of Photoisomerization Quantum Yields. A 1-mm light path-length quartz cell was used for the photoisomerization measurements. The concentrations of the samples were 1×10^{-4} M for dinuclear complexes and 2×10^{-4} M for mononuclear complexes, and the sample solution was degassed by N_2 bubbling before photoirradiation. The trans-to-cis photoisomerization obeyed the first-order kinetics, with the isomerization rate constant, k_{iso}, being evaluated from the change in absorbance by the following equation:[13]

$$\ln \{(A_0 - A_\infty)/(A_t - A_\infty)\} = k_{iso}t \quad (1)$$

where A_0, A_t, and A_∞ denote the absorbance at time $t = 0$, t, and ∞, respectively. Both k_{iso} and A_∞ were evaluated by a nonlinear least-squares calculation. To correct the influence of the change in light intensity of Hg lamps, we measured the isomerization rates of azobenzene in acetonitrile (MeCN) before and after measuring the complexes, and we adopted the ratios in the rate constants of the complexes to azobenzene to compare the isomerization rates. The photoisomerization rate of azobenzene in MeCN was found to be 7.04×10^{-3} s^{-1} at a light intensity of 0.11 W. Quantum yields of photoisomerization ($\Phi_{t\rightarrow c}$) for di-Rhtpy·$6PF_6$ and mono-Rhtpy·$3PF_6$ in dimethyl sulfoxide (DMSO) were determined by using $K_3[Fe(C_2O_4)_3]$ as a chemical actinometer, from the absorbance changes within 10% trans-to-cis structural change. We estimated the $\Phi_{t\rightarrow c}$ values of the complexes in other conditions by assuming that the photoisomerization rate was proportional to $\Phi_{t\rightarrow c}$ for the di-Rhtpy and mono-Rhtpy families, respectively, since their UV−vis absorption spectra do not significantly depend on the solvent and counterion.

Femtosecond Transient Absorption Spectra. The arrangement for the femtosecond pump−probe experiment was essentially the same as that reported elsewhere.[12] Briefly, the laser system consisted of a hybridly mode-locked, dispersion-compensated femtosecond dye laser (Coherent, Satori 774) and a dye amplifier (Continuum, RGA 60−10 and PTA 60). The dye laser (gain dye Pyridine 2 and saturable absorber DDI) was pumped with a cw mode-locked Nd:YAG laser (Coherent, Antares 76S). The sample was excited by the second harmonic (360 nm) of the fundamental (center wavelength 720 nm, pulse width ~200 fs fwhm) at a repetition rate of 10 Hz. The residual portion of the fundamental output was focused on a 1-cm H_2O cell to generate a femtosecond supercontinuum probe pulse. The planes of polarization of the pump and probe beams were set to the magic angle (54.7) to avoid any anisotropic contribution to the transient signal. Both the beams were focused on the sample in a 2-mm cuvette at an angle of less than 5°. Transient spectra were obtained by averaging over 200 pulses and analyzed by an intensified multichannel detector (Princeton Instruments, ICCD-576) as a function of the probe-delay time. The spectra were corrected for the intensity variations and time dispersions of the supercontinuum. Rise and decay curves at a fixed wavelength were measured with a photodiode-monochromator (Japan Spectroscopic, CT-10) combination. The concentration of the sample for transient absorption spectra was kept within $1-1.5 \times 10^{-4}$ M. The solution was allowed to flow through a 2-mm flow cell using a magnetically coupled gear pump (Micropump, 040−332) to avoid any possibility of sample damage during the transient absorption measurement.

Molecular Orbital Calculations. The molecular structures of the complexes were optimized by the MM+ method with the default parameters packaged in the computer program HyperChem Release 6 (HyperCube, Inc.). The point groups of the complexes were assumed as follows: [trans-di-Rhtpy]$^{6+}$ and [trans-di-Rutpy]$^{4+}$ were C_{2h}, those of [trans-mono-Rhtpy]$^{3+}$ and [trans-mono-Rutpy]$^{2+}$ were C_s, and those of $[Rh(tpy)_2]^{3+}$ and $[Ru(tpy)_2]^{2+}$ were D_{2d}. Semiempirical molecular orbital calculations were carried out using the ZINDO/1 method with the same program using default parameters.

Syntheses

tpy-AB. 4′-(4-Anilino)-2,2′:6′,2″-terpyridine (1.3 g, 4.0 mmol) was dissolved in acetic acid (10 mL). After the addition of nitrosobenzene (0.48 g, 4.5 mmol), the solution was stirred overnight. Water (20 mL) was added to the reaction mixture, and the acidic mixture was neutralized with sodium carbonate. The products were extracted with chloroform (300 mL) and separated by column chromatography (Al_2O_3/$CHCl_3$−diethylamine 20:1 eluent). The first orange band was collected, evaporated, and orange powders were obtained; yield 0.79 g (48%). Anal. Calcd for $C_{27}H_{19}N_5$·$1/4H_2O$: C, 77.59; H, 4.70; N, 16.75. Found: C, 77.35; H, 4.66; N, 16.72. ^{1}H NMR ($CDCl_3$): δ 8.79 (s, 2H), 8.73 (d, 2H, $J = 4.0$ Hz), 8.68 (d, 2H, $J = 16.8$ Hz), 8.06 (s, 4H), 7.95 (dd, 2H, $J = 8.3$, 1.7 Hz), 7.88 (td, 2H, $J = 7.9$, 2.0 Hz,), 7.57−7.48(m, 3H); 7.35(ddd, 2H, $J = 8.6$, 4.6, 1.0 Hz). FAB MS (*m*/*z*): 414 $(M + H)^+$.

A General Synthetic Procedure for [(Rhtpy)$_2$(tpy-AB-tpy)]X_6 (di-Rhtpy·6X; X = PF_6, BF_4, BPh_4, TFB, TFPB) and [tpyRh(tpy-AB)]-X_3 (mono-Rhtpy·3X, X=PF_6, BF_4, BPh_4). A mixture of $RhCl_3$tpy (0.071 g, 0.14 mmol), $AgCF_3SO_3$ (0.15 g, 0.59 mmol), and *N*,*N*-dimethylacetamide (6 mL) was refluxed for 1 h. After the solution was cooled to room temperature and filtered, tpy-AB-tpy (0.047 g, 0.072 mmol) was added to the filtrate and the solution was refluxed for 2 h. After being cooled to room temperature and filtered, an excess amount of the salt of the given counterion, NH_4PF_6, NH_4BF_4, $NaBPh_4$, NaTFB, or NaTFPB, in water (30 mL) was added to the solution. The precipitate was collected by filtration and recrystallized from acetonitrile−ether to yield orange-brown products with each counteranion. The mononuclear complexes, [tpyRh(tpy-AB)]X_3, were prepared in a method similar to that used with di-Rhtpy·$6PF_6$ except for using tpy-AB instead of tpy-AB-tpy.

[(Rhtpy)$_2$(tpy-AB-tpy)](PF_6)$_6$ (di-Rhtpy·$6PF_6$). Yield: 68%. Anal. Calcd for $C_{72}H_{50}N_{14}Rh_2$·$6PF_6$·$3H_2O$: C, 38.59; H, 2.51; N, 8.75; Found: C, 38.97; H, 2.51, N, 8.38. ^{1}H NMR (CD_3CN): δ 9.20 (s, 2H), 9.19 (d, 2H, $J = 3.1$ Hz), 8.93−8.90 (m, 6H), 8.80−8.78 (m, 4H), 8.64 (d, 4H, $J = 8.0$ Hz), 8.50−8.41 (m, 8H), 8.34−8.27 (m, 8H), 7.76 (d, 4H, $J = 4.9$ Hz), 7.64 (d, 4H, $J = 5.1$ Hz), 7.56−7.51 (m, 8H). ESI MS *m*/*z* 948.13 ([di-Rhtpy·$4PF_6$]$^{2+}$ requires 948.05), 583.75 ([di-Rhtpy·$3PF_6$]$^{3+}$ requires 583.71).

[(Rhtpy)$_2$(tpy-AB-tpy)](BF_4)$_6$ (di-Rhtpy·$6BF_4$). Yield: 68%. Anal. Calcd for $C_{72}H_{50}N_{14}Rh_2$·$6BF_4$·$3.5H_2O$: C, 45.49; H, 3.11; N, 10.31; Found: C, 45.72; H, 3.52, N, 10.28. ^{1}H NMR (DMSO): δ 9.75 (s, 4H, $H^{3'}$), 9.29−9.27 (m, 8H, H^3, $H^{3'a}$), 9.09 (t, 2H, $J = 8.1$ Hz, $H^{4'a}$), 9.01 (d, 4H, $J = 7.8$ Hz, H^{3a}), 8.76 (d, 4H, $J = 8.6$ Hz, H^o), 8.49−8.37 (m, 12H, H,[4] H^m, H^{4a}), 7.99 (d, 4H, $J = 5.1$ Hz, H^{6a}), 7.88 (d, 4H, $J = 5.1$ Hz, H^6), 7.63−7.56 (m, 8H, H,[5] H^{5a}). ESI MS *m*/*z* 832.13 ([di-Rhtpy·$4BF_4$]$^{2+}$ requires 832.10), 525.74 ([di-Rhtpy·$3BF_4$]$^{3+}$ requires 525.75), 372.56 ([di-Rhtpy·$2BF_4$]$^{4+}$ requires 372.56), 280.64 ([di-Rhtpy·BF_4]$^{5+}$ requires 280.64).

The cis form was prepared by photoirradiation of the trans-di-Rhtpy·$6BF_4$. ^{1}H NMR (DMSO): δ 9.45 (s, 4H, $H^{3'}$), 9.25 (d, 4H, $J = 8.2$ Hz, $H^{3'a}$), 9.18 (d, 4H, $J = 8.3$ Hz, H^3), 9.07 (t, 2H, $J = 8.2$ Hz, $H^{4'a}$), 8.98 (d, 4H, $J = 7.2$ Hz, H^{3a}), 8.48−8.37 (m, 12H, H,[4] H^m, H^{4a}), 7.97 (d, 4H, $J = 5.4$ Hz, H^6), 7.83 (d, 4H, $J = 4.5$ Hz, H^{6a}), 7.58−7.54 (m, 8H, H,[5] H^{5a}), 7.14 (d, 4H, $J = 8.6$ Hz, H^o).

[(Rhtpy)$_2$(tpy-AB-tpy)](BPh_4)$_6$ (di-Rhtpy·$6BPh_4$). Yield: 44%. Anal. Calcd for $C_{216}H_{170}N_{14}B_6Rh_2$·$6H_2O$: C, 77.66; H, 5.49; N, 5.86; Found: C, 77.38; H, 5.41, N, 6.27.^{1}H NMR (CD_3CN): δ 8.99 (s, 4H), 8.77−8.68 (m, 8H), 8.50−8.44 (m, 8H), 8.31−8.26 (m, 6H), 8.11 (td, 8H, $J = 8.4$, 1.7 Hz), 7.56 (d, 4H, $J = 5.4$ Hz), 7.48 (d, 4H, $J = 5.4$ Hz), 7.29−7.26 (m, 8H), 7.23−7.16 (m, 48H), 6.88 (t, 48H, $J = 7.4$ Hz), 6.73 (t, 24H, $J = 7.1$ Hz). ESI MS *m*/*z* 658.13 ([di-Rhtpy]$^{2+}$ requires 658.12), 438.74 ([di-Rhtpy]$^{3+}$ requires 438.75), 329.06 ([di-Rhtpy]$^{4+}$ requires 329.06), 263.26 ([di-Rhtpy]$^{5+}$ requires 263.25), 219.38 ([di-Rhtpy]$^{6+}$ requires 219.38).

[(Rhtpy)$_2$(tpy-AB-tpy)](TFB)$_6$ (di-Rhtpy·6TFB). Yield: 60%. Anal. Calcd for $C_{216}H_{146}N_{14}B_6F_{24}Rh_2$·$3DMA$·$3H_2O$: C, 69.12; H, 4.50;

(12) (a) Tamai, N.; Masuhara, H. *Chem. Phys. Lett.* **1992**, *191*, 189. (b) Mitra, S.; Tamai, N. *Chem. Phys. Lett.* **1998**, *282*, 391.
(13) Gille, K.; Knoll, H.; Quitsch, K. *Int. J. Chem. Kinet.* **1999**, *31*, 337.

N, 6.01. Found: C, 68.86; H, 4.38; N, 5.76. ^{1}H NMR (CD_3CN): δ 9.12 (d, 4H, J = 5.1 Hz), 8.87−8.82 (m, 6H), 8.68 (d, 4H, J = 8.9 Hz), 8.58 (d, 4H, J = 8.4 Hz), 8.41−8.34 (m, 8H), 8.28−8.23 (m, 8H), 7.69 (d, 4H, J = 6.5 Hz), 7.59 (d, 4H, J = 5.5 Hz), 7.49−7.43 (m, 8H), 7.21−7.06 (m, 48H), 6.73 (td, 48H, J = 8.4, 1.9 Hz). ESI MS m/z 658.14 ([di-Rhtpy]$^{2+}$ requires 658.12).

[(Rhtpy)$_2$(tpy-AB-tpy)](TFPB)$_6$ (di-Rhtpy·6TFPB). Yield: 54%. Anal. Calcd for $C_{264}H_{122}N_{14}B_6F_{144}Rh_2$·2DMA: C, 48.97; H, 2.11; N, 3.36. Found: C, 48.75; H, 2.50; N, 3.44. ^{1}H NMR (CD_3CN): δ 9.10 (s, 4H), 8.87−8.79 (m, 6H), 8.69 (d, 4H, J = 8.6 Hz), 8.56 (d, 4H, J = 8.9 Hz), 8.39−8.30 (m, 8H), 8.26−8.17 (m, 8H), 7.88 (d, 4H, J = 7.6 Hz), 7.60−7.57 (m, 76H), 7.45−7.39 (m, 8H). ESI MS m/z 1302.12 ([di-Rhtpy·3TFPB]$^{3+}$ requires 1302.15), 760.85 ([di-Rhtpy·2TFPB]$^{4+}$ requires 760.84), 436.05 ([di-Rhtpy·1TFPB]$^{5+}$ requires 436.06), 329.04 ([di-Rhtpy]$^{4+}$ requires 329.06), 263.24 ([di-Rhtpy]$^{5+}$ requires 263.25).

[tpyRh(tpy-AB)](PF$_6$)$_3$ (mono-Rhtpy·3PF$_6$). Yield: 81%. Anal. Calcd for $C_{42}H_{30}N_8F_{18}P_3Rh$: C, 42.59; H, 2.55; N, 9.46. Found: C, 42.37; H. 2.65; N, 9.31. ^{1}H NMR (CD_3CN): δ 9.17 (s, 2H), 8.91−8.87 (m, 3H), 8.76 (d, 2H, J = 7.3 Hz), 8.62 (d, 2H, J = 7.3 Hz), 8.42 (d, 2H, J = 8.9 Hz), 8.33−8.27 (m, 6H), 8.05−8.02 (m, 2H), 7.73 (d, 2H, J = 5.9 Hz), 7.68−7.61 (m, 5H), 7.53−7.47 (m, 4H). ESI MS m/z 1038.63 ([mono-Rhtpy·2PF$_6$]$^+$ requires 1039.59), 447.00 ([mono-Rhtpy·1PF$_6$]$^{2+}$ requires 447.32).

[tpyRh(tpy-AB)](BF$_4$)$_3$ (mono-Rhtpy·3BF$_4$). Yield: 75%. Anal. Calcd for $C_{42}H_{30}N_8B_3F_{12}Rh$·3/2$H_2O$: C, 48.64; H, 3.21; N, 10.80. Found: C, 48.65; H, 3.42; N, 10.62. ^{1}H NMR (CD_3CN): δ 9.20 (s, 2H), 8.95−8.91 (m, 3H), 8.80 (d, 2H, J = 7.9 Hz), 8.66 (d, 2H, J = 7.9 Hz), 8.45 (d, 2H, J = 8.5 Hz), 8.34−8.28 (m, 6H), 8.05 (dd, 2H, J = 8.2, 2.0 Hz), 7.77 (d, 2H, J = 5.6 Hz), 7.70−7.64 (m, 5H), 7.54−7.51 (m, 4H). ESI MS m/z 923.18 ([mono-Rhtpy·2PF$_6$]$^+$ requires 923.28), 418.12 ([mono-Rhtpy·1PF$_6$]$^{2+}$ requires 418.24).

[tpyRh(tpy-AB)](BPh$_4$)$_3$ (mono-Rhtpy·3BPh$_4$). Yield: 55%. Anal. Calcd for $C_{114}H_{90}N_8B_3Rh$·4H_2O: C, 76.95; H, 5.55; N, 6.30. Found: C, 77.25; H, 5.71; N, 6.05. ^{1}H NMR (CD_3CN): δ 9.09 (s, 2H), 8.81−8.70 (m, 3H), 8.61 (d, 2H, J = 7.6 Hz), 8.47 (d, 2H, J = 8.1 Hz), 8.38 (d, 2H, J = 8.1 Hz), 8.29 (d, 2H, J = 8.1 Hz), 8.17 (dd, 4H, J = 7,3, 1.5 Hz), 8.06−8.02 (m, 2H), 7.67−7.64 (m, 5H), 7.52 (d, 2H, J = 5.1 Hz), 7.40−7.34 (m, 4H), 7.29−7.23 (m, 24H), 6.96 (t, 24H, J = 7.3 Hz), 6.80 (t, 12H, J = 7.3 Hz). ESI MS m/z 749.12 ([mono-Rhtpy]$^+$ requires 749.16), 374.58 ([mono-Rhtpy]$^{2+}$ requires 374.58), 249.69 ([mono-Rhtpy]$^{3+}$ requires 249.72).

A General Method for [(Rhtpy)$_2$(tpy-AB-tpy)]X$_6$ (X = Cl, Br, I). The crude product of [(Rhtpy)$_2$(tpy-AB-tpy)](PF$_6$)$_6$ was dissolved in acetone, and excess tetrabutylammonium halide in acetone was added to the solution. The precipitate was filtered and recrystallized from acetonitrile−ether.

[(Rhtpy)$_2$(tpy-AB-tpy)]Cl$_6$ (di-Rhtpy·6Cl). Yield: 52%. Anal. Calcd for $C_{72}H_{50}N_{14}Cl_6Rh_2$·6$H_2O$: C, 52.80; H, 3.82; N, 11.97. Found: C, 52.72; H, 3.80; N, 12.32. ^{1}H NMR (D_2O): δ 9.26 (s, 4H), 8.92−8.78 (m, 6H), 8.75 (d, 4H, J = 8.2 Hz), 8.64 (d, 4H, J = 8.9 Hz), 8.36−8.18 (m, 16H), 7.71 (d, 4H, J = 4.6 Hz), 7.65 (d, 4H, J = 5.3 Hz), 7.47−7.45 (m, 8H). ESI MS m/z 474.36 ([di-Rhtpy·3Cl]$^{3+}$ requires 474.38), 346.55 ([di-Rhtpy·2Cl]$^{4+}$ requires 346.55), 270.23 ([di-Rhtpy·1Cl]$^{5+}$ requires 270.24).

[(Rhtpy)$_2$(tpy-AB-tpy)]Br$_6$ (di-Rhtpy·6Br). Yield: 63%. Anal. Calcd for $C_{72}H_{50}N_{14}Br_6Rh_2$·3$H_2O$: C, 46.73; H, 3.05; N, 10.60. Found: C, 46.89; H, 3.39; N, 10.84. ^{1}H NMR (D_2O): δ 9.26 (s, 4H), 8.92−8.86 (m, 6H), 8.75 (d, 4H, J = 7.9 Hz), 8.64 (d, 4H, J = 8.6 Hz), 8.37−8.19 (m, 16H), 7.71 (d, 4H, J = 6.0 Hz), 7.65 (d, 4H, J = 5.3 Hz), 7.50−7.43 (m, 8H). ESI MS m/z 518.96 ([di-Rhtpy·3Br]$^{3+}$ requires 519.00), 369.01 ([di-Rhtpy·2Br]$^{4+}$ requires 369.02), 279.40 ([di-Rhtpy·1Br]$^{5+}$ requires 279.43).

[(Rhtpy)$_2$(tpy-AB-tpy)]I$_6$ (di-Rhtpy·6I). Yield: 50%. This complex was not soluble enough in any deuterized solvents to measure the ^{1}H NMR spectrum. Anal. Calcd for $C_{72}H_{50}N_{14}I_6Rh_2$·3$H_2O$·DMA: C, 41.12; H, 2.95; N, 9.46. Found: C, 40.93; H, 3.17; N, 9.09. ESI MS m/z 438.76 ([di-Rhtpy]$^{3+}$ requires 438.75), 329.06 ([di-Rhtpy]$^{4+}$ requires 329.06), 288.64 ([di-Rhtpy·1Br]$^{5+}$ requires 288.63), 263.24 ([di-Rhtpy]$^{5+}$ requires 263.25), 219.37 ([di-Rhtpy]$^{6+}$ requires 219.38).

[tpyRu(tpy-AB)](PF$_6$)$_2$ (mono-Rutpy·2PF$_6$) The complex was prepared according to the literature[8a]; yield 44%. Anal. Calcd for $C_{42}H_{30}N_8F_{12}P_2Ru$·4$H_2O$: C, 48.61; H, 2.91; N, 10.80. Found: C, 48.37; H, 3.05; N, 10.62. ^{1}H NMR (CD_3CN): δ 9.06 (s, 2H), 8.75 (d, 2H, J = 8.3 Hz), 8.66 (d, 2H, J = 7.9 Hz), 8.49 (d, 2H, J = 7.6 Hz), 8.44−8.39 (m, 3H), 8.27 (d, 2H, J = 8.6 Hz), 8.04−8.01 (m, 2H), 7.93 (ddd, 2H, J = 17.3, 7.6, 1.7 Hz), 7.69−7.63 (m, 3H), 7.43 (d, 2H, J = 4.6 Hz), 7.35 (d, 2H, J = 4.3 Hz), 7.17 (t, 4H, J = 6.6 Hz). ESI MS m/z 893.07 ([mono-Rutpy·1PF$_6$]$^+$ requires 892.79), 374.09 ([mono-Rutpy]$^{2+}$ requires 373.92).

Results and Discussion

Synthesis and Characterization. The asymmetrical ligand, tpy-AB, was prepared by the method described elsewhere.[14] While tpy-AB-tpy is soluble only in limited solvents such as chloroform, benzonitrile (PhCN), and *N*,*N*-dimethylformamide (DMF), tpy-AB is soluble in various solvents such as MeCN, DMSO, and propylene carbonate (PC) in addition to the solvents just listed. The Rh dinuclear complexes of tpy-AB-tpy were successfully prepared by the two-step reaction of $RhCl_3$ with tpy and subsequently with tpy-AB-tpy. We prepared the Rh mononuclear and dinuclear complexes with several kinds of counterions in order to examine the effects of the counterion on the photoisomerization behavior (vide infra). Preparation of the halide (X^-) salts was carried out by the anion-exchange reactions of the PF_6^- salts with $Bu_4N^+X^-$. Yields of the Rh complexes containing BPh_4^- were lower than the others, probably due to the instability of BPh_4^- under oxidative conditions.[15] Most Rh complexes are orange-brown, but the halide salts look slightly reddish. The solubility of the halide salts is lower in almost all organic solvents than that of the other salts, but the halide salts are soluble in water. The mononuclear complexes are more soluble in common organic solvents than are the dinuclear complexes.

All the Ru and Rh complexes of tpy-AB-tpy and tpy-AB were fully characterized by ^{1}H NMR, IR, UV−vis, ESI MS, and elemental analysis. In the ^{1}H NMR spectra of the complexes, signals of the protons attached to the terpyridine moieties appear at lower magnetic fields than those of the free ligands, due to the electron-withdrawing effects of the metal centers.

UV−vis absorption spectra of mono-Rutpy·2PF$_6$, tpy-AB, and $[Ru(tpy)_2]^{2+}$ are shown in Figure 1A, inset. The molar extinction coefficient, ϵ, of the MLCT band for mono-Rutpy·2PF$_6$ at 488 nm is larger than that of $[Ru(tpy)_2]^{2+}$ at 474 nm, suggesting the effect of conjugation between the $[Ru(tpy)_2]^{2+}$ moiety and the azo group in mono-Rutpy·2PF$_6$. A similar tendency is observed in di-Rutpy·4PF$_6$, as shown in Figure 1B, inset. It should be noted that the $\pi-\pi^*$ transition band due to the azo moiety in mono-Rutpy·2PF$_6$ appears around 360 nm as a relatively clear shoulder, while that of di-Rutpy·4PF$_6$ is considerably overlapped with the absorption of the $[Ru(tpy)_2]^{2+}$ moiety.[8a] Contrary to $[Ru(tpy)_2]^{2+}$, $[Rh(tpy)_2]^{3+}$ shows no distinct MLCT or d−d band, whereas a ligand-centered (LC) n−π^* or $\pi-\pi^*$ transition band appears in the UV region, as shown in Figure 2, inset. The LC band and the azo $\pi-\pi^*$ band are distinguishable in di- and mono-Rhtpy complexes.

ESI MS were measured to estimate the strength of the ion-pairing and to identify the products. The intensity ratio of the ion-pair peaks was used for the evaluation of the facileness of the successive loss of counterions.[16] The results summarized in Table 1 indicate that the ion-pairing ability increases in the order

(14) Kersten, H.; Boldt, P. *J. Prakt. Chem.* **1996**, *338*, 129.
(15) (a) Nishida, H.; Takada, N.; Yoshimura, M. *Bull. Chem. Soc. Jpn.* **1984**, *57*, 2600. (b) Strauss, D. A.; Zhang, C.; Tilley, T. D. *J. Organomet. Chem.* **1989**, *369*, C13. (c) Tobita, H.; Ishiyama, K.; Kawano, Y.; Inomata, S.; Ogino, H. *Organometallics* **1998**, *17*, 789.

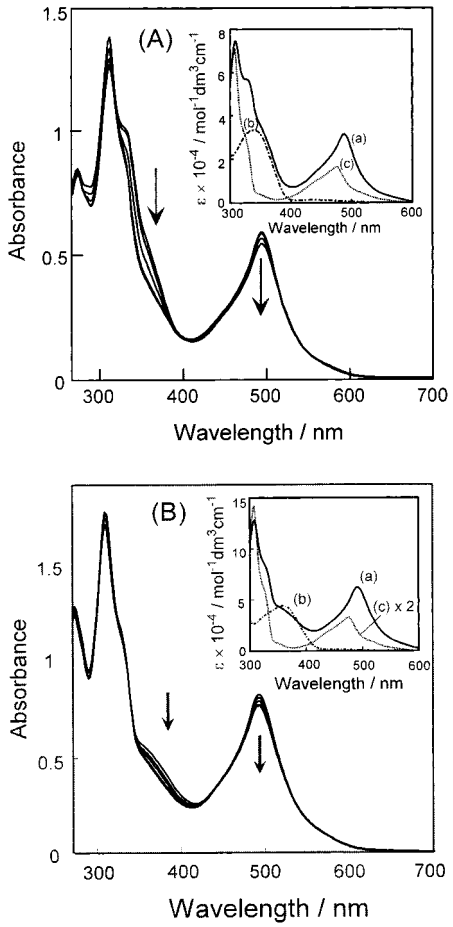

Figure 1. (A) UV−vis spectral change of mono-Rutpy·$2PF_6$ (2.2×10^{-4} M) in DMSO upon irradiation at 366 nm for 1 h. Inset: the spectra of mono-Rutpy·$2PF_6$ (a), tpy-AB (b), and Ru(tpy)$_2$·$2PF_6$ (c). (B) UV−vis spectral change of di-Rutpy·$4PF_6$ (1.3×10^{-4} M) in acetonitrile upon irradiation at 366 nm for 1 h. Inset: the spectra of di-Rutpy·$4PF_6$ (a), tpy-AB-tpy (b), and Ru(tpy)$_2$·$2PF_6$ (c).

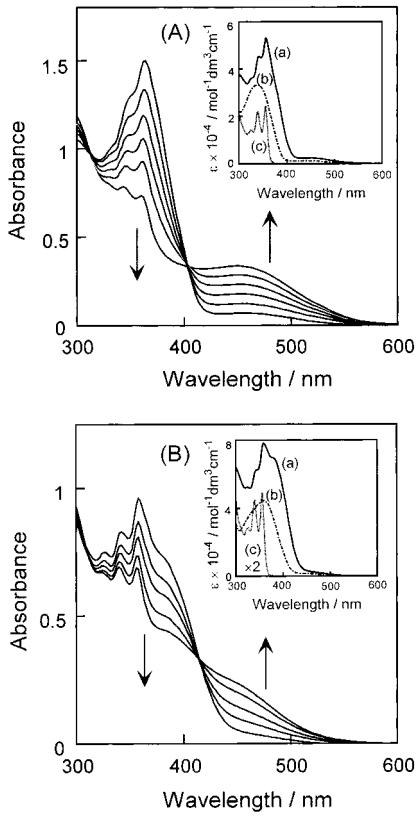

Figure 2. (A) UV−vis spectral change of mono-Rhtpy·$3PF_6$ (2.8×10^{-4} M) in DMSO upon irradiation at 366 nm for 5 min. Inset: the spectra of mono-Rhtpy·$3PF_6$ (a), tpy-AB (b), and Rh(tpy)$_2$·$3PF_6$ (c). (B) UV−vis spectral change of di-Rhtpy·$6PF_6$ (1.1×10^{-4} M) in PC upon irradiation at 366 nm for 40 min. Inset: the spectra of di-Rhtpy·$6PF_6$ (a), tpy-AB-tpy (b), and Rh(tpy)$_2$·$3PF_6$ (c).

di-Rhtpy·$6BPh_4$ < di-Rhtpy·6TFB < di-Rhtpy·6TFPB < halide < di-Rhtpy·$6PF_6$ < di-Rhtpy·$6BF_4$. The BPh_4 salt shows no ion-pair peaks, but instead there is a successive reduction of the complex cation. We compared these ion-pairing effects with the photoisomerization behavior.

Photochemistry of the Ligands and the Ru Complexes. Before studying the photochemistry of the complexes, we examined the isomerization reactions of both free ligands, tpy-AB-tpy[8a] and tpy-AB, in chloroform. Trans-to-cis isomerization occurs upon 366-nm light irradiation excited at the azo $\pi-\pi^*$ transition, and cis-to-trans isomerization occurs upon 450-nm light irradiation excited at the azo $n-\pi^*$ transition. The slow thermal cis-to-trans isomerization of the ligands proceeds at room temperature in the dark. These isomerization behaviors are similar to those of organic azobenzene derivatives.

The photochemical behavior of Ru and Rh complexes was very different from that of free ligands. Upon irradiation at 366 nm, a dinuclear Ru complex, di-Rutpy·$4PF_6$, exhibits no significant change in UV−vis absorption and ^{1}H NMR spectra,[8a] whereas a mononuclear complex, mono-Rutpy·$2PF_6$, exhibits

Table 1. ESI MS Data of Rh Dinuclear (di-Rhtpy) Complexes with Different Counterions

counterion	pattern	intensity
BF_4^-	$[\text{di-Rhtpy}\cdot 4BF_4]^{2+}$	0.67
	$[\text{di-Rhtpy}\cdot 3BF_4]^{3+}$	36
	$[\text{di-Rhtpy}\cdot 2BF_4]^{4+}$	100
	$[\text{di-Rhtpy}\cdot 1BF_4]^{5+}$	53
PF_6^-	$[\text{di-Rhtpy}\cdot 4PF_6]^{2+}$	67
	$[\text{di-Rhtpy}\cdot 3PF_6]^{3+}$	100
BPh_4^-	$[\text{di-Rhtpy}]^{2+}$	5.8
	$[\text{di-Rhtpy}]^{3+}$	2.6
	$[\text{di-Rhtpy}]^{4+}$	100
	$[\text{di-Rhtpy}]^{5+}$	84
	$[\text{di-Rhtpy}]^{6+}$	1.8
TFB^-	$[\text{di-Rhtpy}]^{2+}$	100
$TFPB^-$	$[\text{di-Rhtpy}\cdot 3TFPB]^{3+}$	65
	$[\text{di-Rhtpy}\cdot 2TFPB]^{4+}$	100
	$[\text{di-Rhtpy}\cdot 1TFPB]^{5+}$	5.3
	$[\text{di-Rhtpy}]^{4+}$	43
	$[\text{di-Rhtpy}]^{5+}$	16
Cl^-	$[\text{di-Rhtpy}\cdot 3Cl]^{3+}$	66
	$[\text{di-Rhtpy}\cdot 2Cl]^{4+}$	77
	$[\text{di-Rhtpy}\cdot 1Cl]^{5+}$	100
Br^-	$[\text{di-Rhtpy}\cdot 3Br]^{3+}$	5.8
	$[\text{di-Rhtpy}\cdot 2Br]^{4+}$	46
	$[\text{di-Rhtpy}\cdot 1Br]^{5+}$	100
I^-	$[\text{di-Rhtpy}\cdot 1I]^{5+}$	20
	$[\text{di-Rhtpy}]^{3+}$	5.1
	$[\text{di-Rhtpy}]^{4+}$	31
	$[\text{di-Rhtpy}]^{5+}$	68
	$[\text{di-Rhtpy}]^{6+}$	100

(16) (a) Aston, P. R.; Brown, C. L.; Chapman, J. R.; Gallagher, R. T.; Stoddart, J. F.; *Tetrahedron Lett.* **1992**, *33*, 7771. (b) Leize, E.; Dorsselare, A. V.; Roland, K.; Lehn, J. -M. *J. Chem. Soc., Chem. Commun.* **1993**, 990. (c) Bitsch, F.; Hegy, G.; Buchecker, C. D.; Leize, E.; Sauvage, J. -P.; Van Dorsselaer, A. *New J. Chem.* **1994**, *18*, 801. (d) Arakawa, R.; Miura, S.; Matsubayashi, G.; Matsuo, T. *Bunseki Kagaku* **1996**, *45*, 619. (e) Ralph, S. F.; Sheil, M. M.; Hick, L. A.; Rodney, J. G.; Sargeson, A. M. *J. Chem. Soc., Dalton Trans.* **1996**, 4417. (f) Marquis −Rigault. A.; Dupond- Gerbais, A.; Baxter, P. N. W.; Van Dorsselaer, A.; Lehn, J. -M. *Inorg. Chem.* **1996**, *35*, 2307.

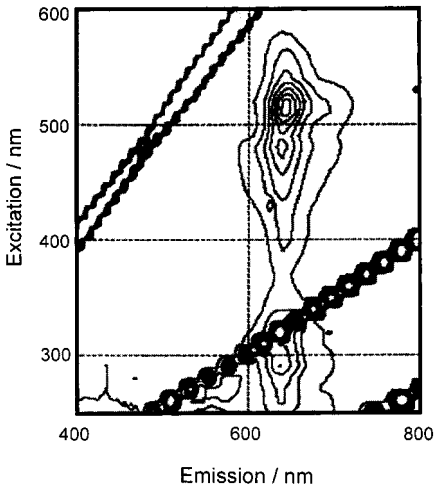

Figure 3. Contour-line plot of excitation−emission spectra of mono-Rutpy·$2PF_6$ in EtOH-MeOH (4:1 v/v) at 77 K.

slight spectral changes according to trans-to-cis isomerization, as shown in Figure 1A. In the photostationary state, the ratio of cis to trans forms was estimated to be 0.21 from the intensity of NMR spectra of the irradiated sample in DMSO-d_6. Figure 3 shows the contour-line plot of the excitation−emission spectrum of mono-Rutpy·$2PF_6$ in frozen EtOH-MeOH (4:1(v/v)) matrix at 77 K. The intensity is much lower than that of $Ru(tpy)_2$·$2PF_6$. It is worth noting that the emission is observed not only by the excitation at the MLCT band around 450 nm but also at the azo $\pi-\pi^*$ transition around 340 nm, while the emission of $Ru(tpy)_2$·$2PF_6$ derives only from the MLCT state. Accordingly, we deduce that suppression of the photoisomerization of the Ru complexes is caused by the energy transfer from the azobenzene moiety to the $[Ru(tpy)_2]^{2+}$ moiety (vide infra). The cis-to-trans backward isomerization of mono-Rutpy·$2PF_6$ occurs slowly in the dark at room temperature, and it is accelerated by the azo $n-\pi^*$ excitation with 440-nm light irradiation.

Trans-to-Cis Photoisomerization of the Rh Complexes and Characterization of the Cis Form. Upon irradiation at 366 nm, all of the mononuclear and dinuclear Rh complexes showed significant UV−vis spectral changes corresponding to the trans-to-cis isomerization, and the absorbance of the $\pi-\pi^*$ transition band decreased and that of the $n-\pi^*$ transition band increased (Figure 2). The photoirradiated products were isolated by precipitation from the DMSO solution by adding 1,4-dioxane. The formation of cis forms was supported by other spectral results of the isolated products, as described below. In the ^1H NMR spectrum of the product from trans-di-Rhtpy·$6BF_4$ in DMSO-d_6, signals of H^3, H,[6a] $H^{3'}$, and H^o (see Chart 1) are shifted to the higher magnetic field by $\Delta\delta = 0.10$, 0.16, 0.30, and 1.62, respectively, and only H^6 is shifted to the lower magnetic field by $\Delta\delta = -0.09$ (see Experimental). This result can possibly be explained by the shorter π-conjugation length and weaker electron-withdrawing effect of the azo moiety in the cis form compared with the trans form, according to the twisted structure around the azo moiety. The magnitude of the shift of signals tends to be more significant for protons closer to the azo moiety, especially for the H^o proton ($\Delta\delta = 1.62$ ppm). In the IR spectra of the cis complexes, a weak absorption of the N=N stretching mode, which is IR-inactive in trans complexes due to their inversion symmetry,[17]appears at 1534 cm^{-1} (Figure 4).

A cyclic voltammogram of di-Rhtpy·$6BF_4$ in Bu_4NBF_4−MeCN displays an irreversible Rh(III)/Rh(I) reduction wave at

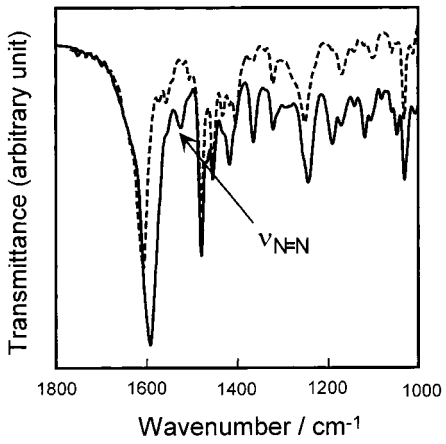

Figure 4. IR spectra of the trans (dotted line) and cis forms (solid line) of di-Rhtpy·$6PF_6$ in a KBr matrix.

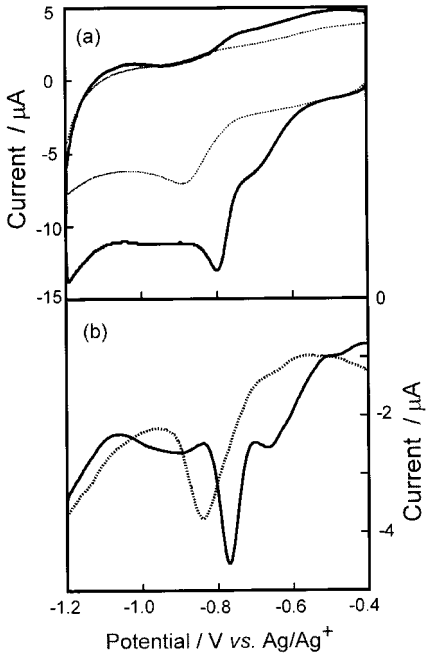

Figure 5. Cyclic voltammograms (a) and differential pulse voltammograms (b) of trans-di-Rhtpy·$6BF_4$ (solid line) and cis-di-Rhtpy·$6BF_4$ (dotted line) in 0.1 M Bu_4NBF_4−MeCN.

−0.80 V for the trans form and another at −0.88 V for the cis form, as shown in Figure 5. Mono-Rhtpy·$3BF_4$ also shows an irreversible Rh(III)/Rh(I) reduction wave at −0.80 V for the trans form and at −0.88 V for the cis form. The lack of difference in the reduction potential between the mononuclear and dinuclear complexes indicates that the internuclear electronic interaction in the dinuclear complex through the azobenzene moiety is negligible. The negative shift of the metal-centered redox potential by the trans-to-cis isomerization suggests that the azo group has less electron-withdrawing effect in the cis form compared with the trans form. This tendency is similar to that of azoferrocene, whereas the potential shift of azoferrocene is 0.3 V, larger than that of the Rh complexes.[18]

Cis-to-Trans Isomerization of the Rh Complexes. Cis-to-trans photoisomerization upon 430-nm light irradiation exciting

(17) (a) Tecklenburg, M. M. J.; Kosnak. D. J.; Bhatnagar, A.; Mohanty, D. K. *J. Raman. Spectrosc.* **1997**, *28*, 755. (b) Hamm. P.; Ohline, S. M.; Zinth, W. *J. Chem. Phys.* **1997**, *106*, 519. (c) Biswas, N.; Umapathy, S. *J. Phys. Chem. A* **2000**, *104*, 2734.

(18) Kurihara, M.; Matsuda, T.; Hirooka, A.; Yutaka, T.; Nishihara, H. *J. Am. Chem. Soc.* **2000**, *122*, 12373.

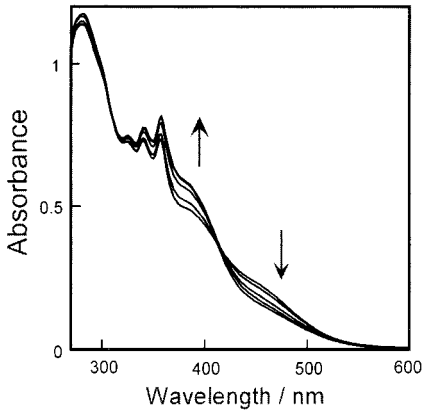

Figure 6. Cis-to-trans UV−vis spectral change of di-Rhtpy·6PF_6 (1.1×10^{-4} M) in PC heating at 120 °C for 12 h.

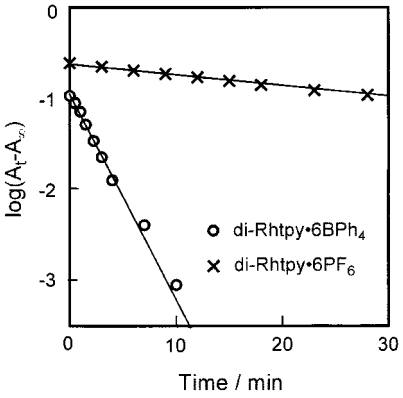

Figure 7. Plots of $\log(A_t - A_\infty)$ vs time for di-Rhtpy·6BPh_4 and di-Rhtpy·6PF_6 in PC upon irradiation at 366 nm.

the azo n−π^* transition was not observed for any of the mononuclear or dinuclear Rh complexes in this study. In contrast, at elevated temperatures in the dark, slow spectral change with the isosbestic point at 420 nm ascribable to the thermal cis-to-trans isomerization occurs (Figure 6). This thermal isomerization is much slower than that of the free ligands. The minimum temperature at which the isomerization occurred in PC for 1 day depends markedly on the type of counterion: 120 °C for the dinuclear Rh complexes containing PF_6^- and BF_4^-, above 90 °C for those containing Cl^-, Br^-, and I^-, and 25 °C for those containing BPh_4^-, TFB^-, and $TFPB^-$.

We considered the contribution of the ion-paring ability to the apparent volume of the complexes with regard to the counterion effects. The dependence of the ion-pairing strength of the complex cation on the counterion was evaluated based on the ESI MS spectral data given in Table 1. The electrostatic interaction between the complex cation and the counterion is weaker for BPh_4^- than BF_4^- and PF_6^-, and the order among them is consistent with the tendency of the cis-to-trans isomerization temperature. This phenomenon can be interpreted as follows: the largeness of the anions leads to the weaker electrostatic interaction between the complex cations and the counterions and the smaller apparent rotor volume of the complex cation around the azo group for isomerization. The other anions form ion pairs with the complex cation more easily, and, thus, the rotor volume of the complex is larger than that of the free cation by itself due to the contribution of the anions. Complexes containing halide ions were isomerized at lower temperatures than those containing PF_6^- or BF_4^-, probably because halide ions are smaller than PF_6^- or BF_4^-, leading to a smaller rotor volume of the complex.

Mono-Rhtpy complexes also underwent the thermal cis-to-trans isomerization, depending on the counterions. The temperature showing a significant spectral change for 1 day is 25 °C for the BPh_4^- salt and above 120 °C for the PF_6^- and BF_4^- salts. Compared with the thermal cis-to-trans isomerization rate constants of tpy-AB-tpy (7.9×10^{-4} s^{-1} at 50 °C) in DMF and organic azobenzenes given in the literature,[9] the rate constant of di-Rhtpy·6BPh_4 in DMF is much smaller (6.7×10^{-7} s^{-1} at 50 °C).

Quantum Yields of the Trans-to-Cis Photoisomerization. The absorption spectral change in the initial stage of the photoisomerization follows the first-order reaction kinetics, as shown in Figure 7, due to the quite slow photo- and thermal cis-to-trans isomerization, as mentioned above. Quantum yields of the trans-to-cis photoisomerization were measured for mono- and dinuclear Rh complexes with various counterions in several solvents such as PhCN, MeCN, DMF, *N*,*N*-dimethylacetamide (DMA), DMSO, and PC with different physical properties. The results given in Table 2 indicate that the $\Phi_{t\rightarrow c}$ values of the Rh complexes are below 0.006, much less than those of the organic azobenzenes ($\Phi_{t\rightarrow c} = 0.1-0.2$).[19]

The quantum yield is strongly dependent on the counterions, as shown in Table 3. The photoisomerization of di-Rhtpy·6BPh_4 is more efficient than that of di-Rhtpy·6PF_6 and di-Rhtpy·6BF_4. Di-Rhtpy·6BPh_4 was subject to trans-to-cis photoisomerization even in the KBr pellet, while the free ligand did not exhibit significant isomerization behavior in the KBr pellet. We note again the contribution of the ion-paring ability to the apparent volume of the complexes with regard to the counterion effects on the photoisomerization. The electrostatic interaction between the complex cation and the counterion evaluated from the ESI MS data is consistent with the tendency of $\Phi_{t\rightarrow c}$, indicating that the anion with the lower ion-pairing ability reduces the apparent rotor volume for the isomerization, resulting in a more facile isomerization. As for the complexes containing tetraarylborate ions, no ion-pairing peaks were detected by ESI MS except for the TFPB salt, and thus the ion-pairing strength is estimated to be in the order $BPh_4^- \approx TFB^- \ll TFPB^-$. This order is the reverse of the order of $\Phi_{t\rightarrow c}$, $TFPB^- \ll TFB^- < BPh_4^-$. We therefore concluded that the electron-withdrawing effect of substituted fluorine atoms causes the stronger ion pairing, which plays a negative role in photoisomerization. As for the complexes with halide ions, the $\Phi_{t\rightarrow c}$ value increases in the order of $I^- < Br^- < Cl^-$. This order seems contradictory to the order estimated from the ion-pairing strength, $I^- < Br^- < Cl^-$. In this case, we deduce that the ion pairing with halide ions is somewhat stronger than that with other anions because of the smaller ion size, and the difference in ion-paring strength among the halide ions is not significant. As a result, the increase in the size of the halide ions, $Cl^- < Br^- < I^-$, largely contributes to the increase of the apparent rotor volume.

The photochemical or thermal isomerization of symmetrical or less polar organic azobenzenes is not affected by the polarity of the solvents.[4,9a,9b] In the present study, however, significant solvent effects were observed on the photoisomerization kinetics of the Rh complexes (see Table 2). The first notable effect is

(19) (a) Birnbaum. P. P.; Style, D. W. G. *Trans. Faraday Soc.* **1954**, *50*, 1192 (b) Malkin, S.; Fischer, E. *J. Phys. Chem.* **1962**, *66*, 2482. (c) Gegiou, D.; Muszkat, K. A.; Fischer, E. *J. Am. Chem. Soc*. **1968**, *90*, 3907. (d) Ronayette, J.; Arnaud. R.; Lebourgeois. P.; Lemaire, J. *Can. J. Chem.* **1974**, *52*, 1848. (e) Bortolus, P.; Monti, S. *J. Phys. Chem.* **1979**, *83*, 648. (f) Rau, H. *J. Photochem.* **1984**, *26*, 221. (f) Rau, H.; Yu-Quan, S, *J. Photochem. Photobiol. A* **1988**, *42*, 321. (g) Lednev, I. K.; Ye, T. -Q.; Abbott, L. C.; Hester, R. E.; Moore, J. N. *J. Phys. Chem. A* **1998**, *102*, 9161.

Table 2. Quantum Yields of Dinuclear and Mononuclear Rh Complexes Dependent on Various Solvents and Counterions

			$10^3\Phi_{t\rightarrow c}$					
solvent	dielectric constant ϵ[a]	viscosity (η/mPa s)[a]	di-Rhtpy·6BF_4	di-Rhtpy·6PF_6	di-Rhtpy·6BPh_4	mono-Rhtpy·3BF_4	mono-Rhtpy·3PF_6	mono-Rhtpy·3BPh_4
PhCN	25.9	1.27	0.34	0.062	3.9	0.29	*b*	*b*
MeCN	36.6	0.369	0.016	0.011	5.1	*b*	*b*	5.7
DMF	38.3	1.794	3.4	3.9	5.5	2.7	2.9	2.3
DMA	38.9	1.96	3.5	4.4	5.4	4.2	4.0	4.2
DMSO	47.2	1.99	0.58	1.6	3.3	1.9	1.6	2.1
PC	68.8	2.53	0.052	0.11	1.5	0.042	*b*	0.25

[a] Lide, D. R. *CRC Handbook of Chemistry and Physics*, 79th ed.; CRC Press, 1998. [b] No significant photoisomerization behavior was observed ($\Phi_{t\rightarrow c} < 10^{-6}$).

Table 3. Quantum Yields of Dinuclear Rh Complexes with Different Counterions in PC

counterion	$10^3\Phi_{t\rightarrow c}$
BF_4	0.054
PF_6	0.11
BPh_4	1.5
TFB	0.96
TFPB	0.32
Cl	0.28
Br	0.12
I	0.11

Table 4. Trans-to-Cis Photoisomerization Rate of Di-Rhtpy·6PF_6 with Triplet Photosensitizers in PC

photosensitizer	E_t (kJ mol^{-1})[a]	relative rate constant
acetophenone	310	1
benzophenone	287	14
anthraquinone	261	25
benzil	223	1
no sensitizer		1

[a] Murov, S. L.; Carmichael, I.; Hug, G. L.; *Handbook of Photochemistry*; New York: Dekker, 1993.

the solvation to the cationic form of the Rh(III) complexes. Stronger solvation of the complex cations occurs in more polar solvents, and it leads to an enlargement of the apparent rotor volume of the complex. The second notable effect is to weaken the electrostatic interaction between the complex cation and the counterion by the strong solvation to both ions, which results in the decrease in the apparent rotor volume of the complex. The complicated dependence of $\Phi_{t\rightarrow c}$ on the solvent would be due to the combination of these two opposite solvent effects. Although the polarity of MeCN, DMF, and DMA can be regarded to be similar judging from their dielectric constants, $\Phi_{t\rightarrow c}$ in these solvents varies over a wide range, especially for PF_6^- and BF_4^- salts. This phenomenon may be due to the structural difference between the N-donor, MeCN, and the O-donor, DMF or DMA. If we make a comparison between the rate constants in similar N-donors, PhCN and MeCN, the $\Phi_{t\rightarrow c}$ value is smaller in more polar MeCN. There have been some reports of a general tendency for the photoisomerization of organic azobenzenes to be depressed in more viscous solutions.[13,20] This tendency may appear as the lowest $\Phi_{t\rightarrow c}$ value in the most viscous PhCN in the series of data for the BPh_4^- salt, and there is little dependency of $\Phi_{t\rightarrow c}$ value on the polarity of the solvent.

The solvent effects on $\Phi_{t\rightarrow c}$ of mono-Rhtpys were basically similar to those of di-Rhtpys. It is notable that mono-Rhtpy showed a small dependence of $\Phi_{t\rightarrow c}$ on the counterion, especially in the solvents where relatively quick photoisomerization occurs (DMA, DMF, DMSO, and PC). This should be due to slight interaction of the counterion of mono-Rhtpy with the neutral azophenyl moiety.

Sensitized Trans-to-Cis Photoisomerization in the Triplet State. Several studies on the triplet-sensitized photoisomerization of olefins[21] and azobenzenes[19d,e,22] have been carried out. In the present study, several kinds of triplet photosensitizers were added to the solution of di-Rhtpy·6PF_6 in PC, and the photoisomerization rates were obtained by a method similar to that described above. Results are given in Table 4. The photoisomerization reaction of di-Rhtpy·6PF_6 is enhanced by the addition of benzophenone or anthraquinone as a photosensitizer. The photosensitized trans-to-cis isomerization process of di-Rhtpy·6BF_4 with anthraquinone was monitored by ^{1}H NMR spectroscopy in DMSO-d_6. The spectral change demonstrated the trans-to-cis photoisomerization of di-Rhtpy·6BF_4 without change in the signals of anthraquinone. The addition of acetophenone with high triplet energy or benzil with low triplet energy caused no enhancement of photoisomerization. Based on these results, we can expect that the triplet energy of di-Rhtpy·6PF_6 would be approximately 260 kJ mol^{-1}. Although the photoisomerization rates of the Rh complexes by themselves are much lower than those of organic azobenzenes, the rates of the Rh complexes can come close to those of the organic azobenzenes with the addition of the proper triplet photosensitizer. In contrast, we did not observe trans-to-cis triplet-sensitized photoisomerization of the Ru complexes, probably because the efficiency of the energy transfer from the azo $\pi-\pi^*$ excited state to the Ru MLCT state is enhanced by the photosensitizer.

Femtosecond Transient Absorption Spectroscopy. Femtosecond transient absorption spectroscopy has been used for the direct observation of the photoisomerization reaction of azobenzenes.[19g,23] Figure 8 shows femtosecond transient absorption spectroscopy of di-Rhtpy·6PF_6 and di-Rutpy·4PF_6. For the Rh complex, the behavior is similar to that of organic azobenzenes; at first a very broad $S_n \leftarrow S_2$ ($\pi-\pi^*$ state) absorption band at ~500 nm (within 1 ps) appeared and decayed rapidly. Next, an intense $S_n \leftarrow S_1$ (n-π^* state) absorption band at ~450

(20) (a) Asano, T.; Cosstick, K.; Furuta, H.; Matsuo, K.; Sumi, H. *Bull. Chem. Soc. Jpn*. **1996**, *69*, 551. (b) Murarka, R.; Bhattacharyya, S.; Biswas, R.; Bagchi, B. *J. Chem. Phys.* **1999**, *110*, 7365. (c) Denny, R. A.; Bagchi, B. *J. Phys. Chem. A* **1999**, *103*, 9061.

(21) (a) Arai, T.; Karatsu, T.; Sakuragi, H.; Tokumaru, K. *Tetrahedron Lett.* **1983**, *24*, 2873. (b) Sundahl, M.; Wennerström, O.; Sandros, K.; Arai, T.; Tokumaru, K. *J. Phys. Chem.* **1990**, *94*, 6731. (c) Anger, I.; Sundahl, M.; Wennerström, O.; Sandros, K.; Arai, T.; Tokumaru, K. *J. Phys. Chem.* **1992**, *94*, 7027. (d) Arai, T.; Tokumaru, K. *Chem. Rev.* **1993**, *93*, 23. (e) Jonson, H.; Sundahl, M.; *J. Photochem. Photobiol. A* **1996**, *93*, 145.

(22) (a) Ronayette, J.; Arnaud. R.; Lemaire, J. *Can. J. Chem.* **1974**, *52*, 1858. (b) Arnaud. R.; Lemaire, J. *Can. J. Chem.* **1974**, *52*, 1868. (c) Archut A.; Azzellini, G. C.; Balzani, V.; De Cola, L.; Vögtle, F. *J. Am. Chem. Soc.* **1998**, *120*, 12187.

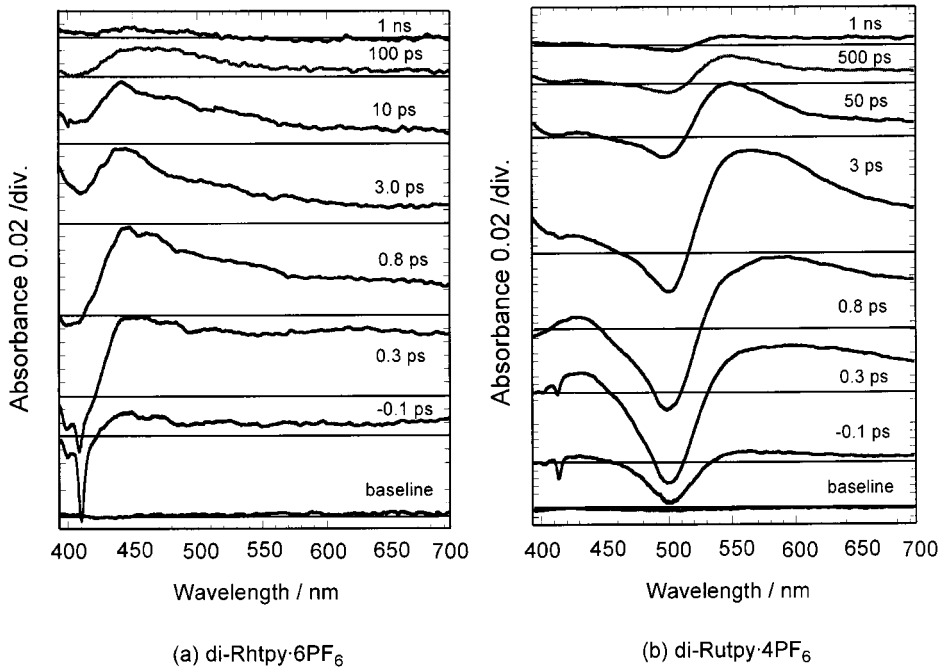

Figure 8. Transient absorption spectra of di-Rhtpy·$6PF_6$ (a) and di-Rutpy·$4PF_6$ (b) in acetonitrile, excited by the second harmonic (360 nm) of the fundamental (center wavelength 720 nm, pulse width ~200 fs fwhm). Each spectrum was obtained by averaging over 200 pulses.

nm (within 2 ps) appeared. The lifetimes of S_2 or S_1 states and the decay dynamics of the complexes are similar to those of organic azobenzenes,[23] in which the trans-to-cis photoisomerization is regarded to occur from the S_1 state even in the excitation to the S_2 state. These results indicate that the photoisomerization of the Rh complex occurs from the S_1 state. For di-Rutpy·$4PF_6$, very fast bleaching of the Ru MLCT band at 500 nm occurred. We also measured the transient absorption spectra of $Ru(tpy)_2$·$2PF_6$ in acetonitrile to analyze the dynamics of the energy transfer. The bleaching signal of the ground state was 10 times smaller for $Ru(tpy)_2$·$2PF_6$ than for di-Rutpy·$4PF_6$. We detected a rise component of 200 fs at the MLCT band of di-Rutpy·$4PF_6$, whereas no rise component was observed for $Ru(tpy)_2$·$2PF_6$. Accordingly, we believe that the azobenzene unit is mainly excited at 360 nm in azobenzene-conjugated Ru complex and that the ultrafast excitation energy transfer from the azobenzene unit to the $Ru(tpy)_2$ unit is responsible for the suppression of the trans−cis photoisomerization. These results support the discussion above.

Molecular Orbital Calculation. Theoretical calculations have been carried out to determine the trans−cis reaction path of azobenzenes,[4,16c,24] and to investigate the photochemistry and energy transfer of the complexes.[25] In the present study, we calculated the molecular orbitals at the optimized structure of the azobenzene, Rh, and Ru complexes (trans form) at the semiempirical ZINDO/1 level. The simple energy diagrams are shown in Figure 9, and the details are shown in Figures 10S and 11S, Supporting Information. The total energy is greatly stabilized by the attachment of the complex unit at the para-position of the azobenzene molecule. As for the Rh complexes, the HOMO is composed of the π-orbital of the azo group, and there are no orbitals related to d-orbitals in the wide energy range below the HOMO level. Accordingly, it appears that the $\pi-\pi^*$ transition of the azo group of mono-Rhtpy and di-Rhtpy complexes is not much affected by the $Rh(tpy)_2$ unit. As for the Ru complexes, although the HOMO is also composed of the π-orbital of the azo group, there is significant contribution of Ru d-orbitals near the HOMO level. Moreover, the energy levels of the azo π^*-orbital and terpyridine ligand π^*-orbital are relatively close, suggesting that the azo $\pi-\pi^*$ and MLCT transitions can interact with each other. These results are consistent with the experimental results noted above.

Conclusion

The Rh mononuclear and dinuclear terpyridine complexes involving an azobenzene undergo trans-to-cis photoisomerization by the direct excitation of the azobenzene unit with 366-nm light. Cis-to-trans isomerization by heat and light occurs in few cases, enabling us to isolate the cis forms of the complexes. The cis form has more negative reduction potentials than the trans form by 80 mV. The photoisomerization quantum yield is strongly dependent on the solvents and counterions. In the case of the Ru complexes, no significant trans-to-cis photoisomerization occurs, indicating that the photoisomerization

(23) (a) Lednev, I. K.; Ye, T. -Q.; Hester, R. E.; Moore, J. N. *J. Phys. Chem.* **1996**, *100*, 13338. (b) Wachtveitl, J.; Nägele, T.; Puell, B.; Zinth, W.; Kruger, M.; Böhner, S. R.; Oesterhelt, D.; Moroder, L. *J. Photochem. Photobiol. A* **1997**, *105*, 283. (c) Lednev, I. K.; Ye, T.-Q.; Matousek, P.; Towrie, M.; Foggi, P.; Neuwahl, F. V. R.; Umapathy, S.; Hester, R. E.; Moore, J. N. *Chem. Phys. Lett.* **1998**, *290*, 68. (d) Azuma, J.; Tamai, N.; Shishido, A.; Ikeda, T. *Chem. Phys. Lett.* **1998**, *288*, 77.

(24) (a) Morley, J. O. *J. Mol. Struct. (THEOCHEM)* **1995**, *340*, 45. (b) Kucharski, S.; Janik, R.; Motschmann, H.; Radüge, C. *New J. Chem.* **1999**, *23*, 765. (c) Shaabani, A.; Zahedi, M. *J. Mol. Struct. (THEOCHEM)* **2000**, *506*, 257. (d) Kurita, N.; Tanaka, S.; Itoh, S. *J. Phys. Chem. A* **2000**, *104*, 8114.

(25) (a) Constable, E. C.; Housecroft, C. E. *Polyhedron* **1990**, *9*, 1939. (b) Calzaferri, G.; Rytz, R.; *J. Phys. Chem.* **1995**, *99*, 12141. (c) Sizova, O. V.; Baranovski, V. I.; Ivanova, N. V.; Panin, A. I. *Int. Quantum Chem.* **1997**, *63*, 853. (d) Rensmo, H.; Lunell, S.; Siegbahn, H. *J. Photochem. Photobiol. A* **1998**, *114*, 117. (e) Constantino, V. R. L.; Toma, H. E.; de Oliveira, L. F.; Rein, F. N.; Rocha, R. C.; de Oliveira, Silva, D. *J. Chem. Soc., Dalton Trans.* **1999**, 1735. (f) Marcaccio, M.; Paolucci, F.; Paradisi, C.; Roffia, S.; Fontanesi, C.; Yellowlees. L. J.; Serroni, S.; Campagna, S.; Denti, G.; Balzani, V. *J. Am. Chem. Soc.* **1999**, *121*, 10081. (g) Rak, J.; Voityuk, A.; Rösch, N. *Int. Quantum Chem.* **2000**, *77*, 128.

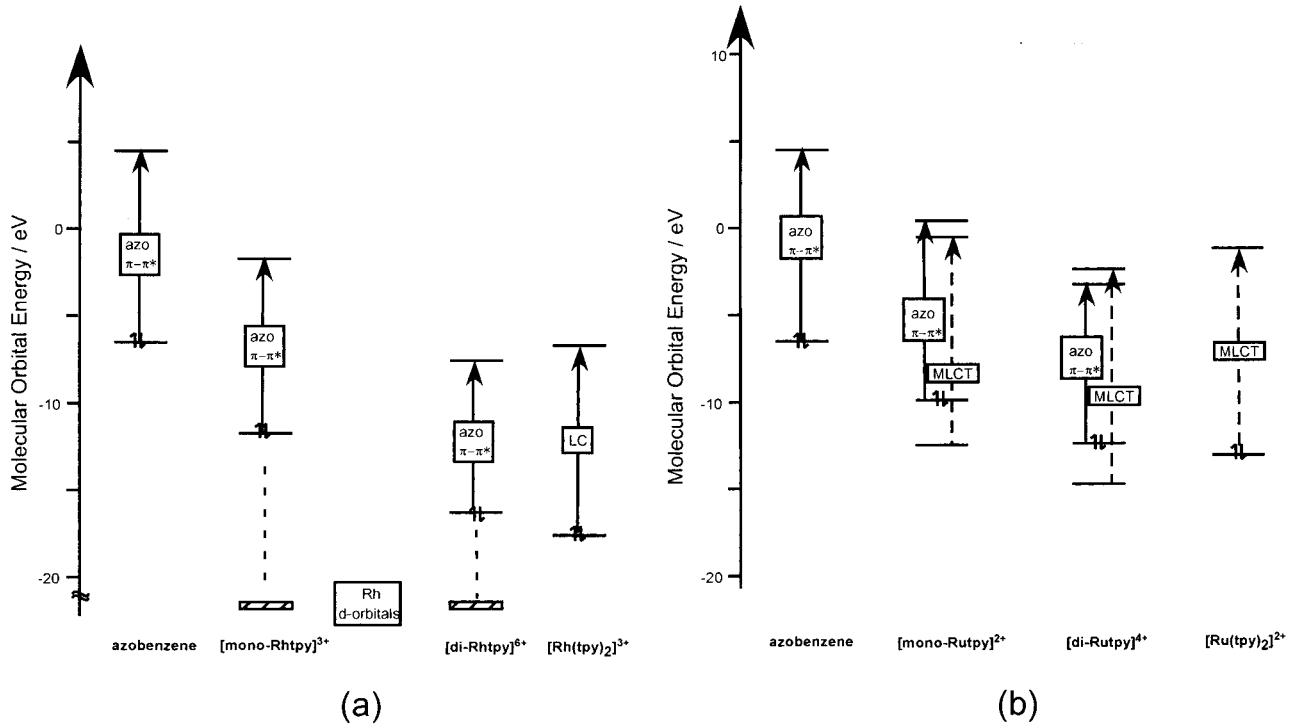

Figure 9. The molecular orbital energy diagram of azobenzene, [mono-Rhtpy]$^{3+}$, [di-Rhtpy]$^{6+}$, and [Rh(tpy)$_2$]$^{3+}$ (a) and that of azobenzene, [mono-Rutpy]$^{2+}$, [di-Rutpy]$^{4+}$, and [Ru(tpy)$_2$] $^{2+}$ (b) estimated from ZINDO calculation.

behavior is strongly dependent on the metal centers. Transient absorption spectroscopy has indicated that the energy transfer pathway to the MLCT of the Ru complex moiety is the primary cause of the depressed photoisomerization.

Acknowledgment. This work was supported by Grants-in-Aid for scientific research (Nos. 10149102, 11167217, and 11309003) from the Ministry of Education, Science, Sports and Culture, Japan, the Tokyo Ohka Foundation, and the Hayashi Memorial Foundation for Female Natural Scientists (to Yutaka).

Supporting Information Available: Molecular orbital energy diagrams of Rh complexes (Figure 10S) and Ru complexes (Figure 11S) calculated by HyperChem 6, using the ZINDO/1 method. This material is available free of charge via the Internet at http://pubs.acs.org.

IC010351U